



Oliver Klaproth

Introduction

The ZEISS IOLMaster 700 with SWEPT Source Biometry® is the latest optical biometer in the more than 20-year long history of biometry innovation from ZEISS (Fig. 17.1). It combines all measurements required for modern IOL power calculation formulas at very precise levels [1]. It combines those with innovative technologies to support the improvement of refractive outcomes such as Total Keratometry (TK®), which enables the use of posterior corneal curvature measurements in IOL power calculation [2–5], the cornea-to-retina scan, the unique fixation check [6], and central topography. The ZEISS IOLMaster 700 is an integral part of the ZEISS

Cataract Workflow, which enables remote IOL power calculation and surgical planning, IOL ordering, and more, in combination ZEISS EQ Workplace® for ZEISS FORUM® and ZEISS Veracity® Surgical software. It also enables markerless toric IOL alignment in combination with ZEISS CALLISTO eye® for surgical microscopes OPMI LUMERA® or ARTEVO® 800. It adheres to applicable DICOM standards and can therefore be networked with EMR and PACS systems. Overall, the ZEISS IOLMaster 700 builds on more than 20 years of experience in optical biometry, delivers precise and reliable measurements, and helps optimizing clinical cataract workflows [2, 3, 7]. It is designed to increase patient throughput and for getting fewer refractive surprises.

O. Klaproth (✉)
ZEISS Ophthalmology, Berlin, Germany
e-mail: oliver.klaproth@zeiss.com

Fig. 17.1 ZEISS IOLMaster 700



SWEPT Source Biometry®

OCT Technology

The ZEISS IOLMaster 700 is a SWEPT Source OCT Biometer that operates at a wavelength from 1035 to 1080 nm with a scanning rate of 2 kHz and 44 mm scan depth, to generate a 2D OCT cornea-to-retina cross-section scan of the eye in six meridians (0°, 30°, 60°, 90°, 120°, and 150°). Each meridional scan is averaged from three single scans. This technology is used to derive all axial biometry measurements, including **axial lengths**, **central corneal thickness**, **anterior chamber depths** from epithelium and endothelium, and **lens thickness**, at very precise levels (Table 17.1) [4, 5, 9–17].

The seamless cornea-to-retina cross-section scan furthermore aids surgeons in detecting unusual eye geometries. In contrast to A-Scan biometers, it furthermore enables to verify the correctness of measurements by displaying the anatomical structures and overlaying the seg-

mentation used for axial measurements (Fig. 17.2).

The ZEISS IOLMaster 700 is designed to optimize workflow efficiency, even when handling dense cataracts.

The combination of SWEPT Source OCT 6-meridian scan pattern and the use of approx. 1055 nm wavelengths (rather than, for example, 1300 nm, which has a higher energy absorption rate in the vitreous) enables a cataract penetration rate of up to 99% [18].

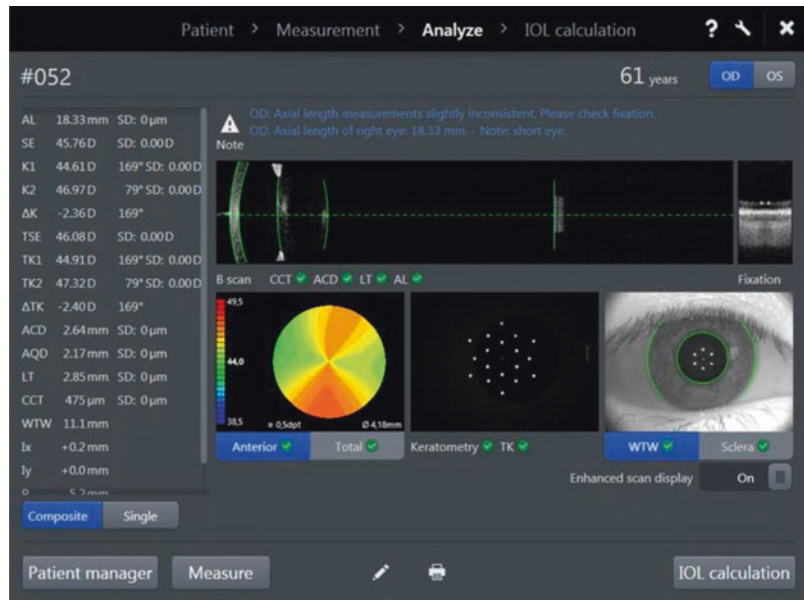
Unique Fixation Check

The ZEISS IOLMaster 700 also utilizes the SWEPT Source OCT to take a horizontal cross section image of the central 1 mm of the macula, which is averaged from 4 scans (Fig. 17.2). This enables users to verify whether the axial lengths and keratometry measurement were taken during correct fixation, to reduce the risk of refractive surprises due to incorrect measurements caused by undetected poor fixation.

Table 17.1 ZEISS IOLMaster 700 technical data

Measurement range	<ul style="list-style-type: none"> • Axial length 14–38 mm • Corneal radii 5–11 mm • Anterior chamber depth 0.7–8 mm • Lens thickness <ul style="list-style-type: none"> – 1–10 mm (phakic eye) – 0.13–2.5 mm (pseudophakic eye) • Central corneal thickness 0.2–1.2 mm • Corneal diameter 8–16 mm
Display scaling	<ul style="list-style-type: none"> • Axial length 0.01 mm • Corneal radii 0.01 mm • Anterior chamber depth 0.01 mm • Lens thickness 0.01 mm • Central corneal thickness 1 μm • Corneal diameter 0.1 mm
SD of repeatability [8]	<ul style="list-style-type: none"> • Axial length 5 μm • Corneal radii 0.09 D • Cylinder >0.75 D, axis 3.8° • Anterior chamber depth 7 μm • Lens thickness 6 μm • Central corneal thickness 2.5 μm • Corneal diameter 111 μm
IOL calculation formulas	<ul style="list-style-type: none"> • See Table 17.2
Interfaces	<ul style="list-style-type: none"> • ZEISS VERACITY surgical • ZEISS EQ workplace • ZEISS EQ Mobile • ZEISS FORUM eye care data management system • ZEISS computer-assisted cataract surgery system CALLISTO eye (via USB, EQ workplace and EQ Mobile, and FORUM) • Data interface for electronic medical record (EMR)/patient management systems (PMS) • Holladay IOL consultant software and PhacoOptics® • Data export to USB storage media, including comprehensive CSV batch export. • Ethernet port for network connection and network printer • Import of IOL data from IOLCon.org
Line voltage	<ul style="list-style-type: none"> • 100–240 V \pm 10%
Line frequency	<ul style="list-style-type: none"> • 50–60 Hz
Power consumptions	<ul style="list-style-type: none"> • Max. 150 VA
Laser class	<ul style="list-style-type: none"> • 1

Fig. 17.2 ZEISS IOLMaster analysis screen, showing measurement values, SS-OCT images, central topography maps, telecentric 3-zone keratometry spots, and CD/reference images, and plausibility checks



Distance Independent Telecentric 3-Zone Keratometry

Telecentric Keratometry utilizes projection of keratometry points on the cornea via a parallel ray system, rather than reflecting divergent light directly from LEDs, thus simulating an infinite light source incident on the precorneal tear film. The light spots are then diffusely reflected by the tear film. Due to an aperture stop placed in the focus of the objective lens in the observation beam path, only the rays parallel to the optical axis are detected by the sensor. A slight change of distance between the cornea and the objective thus has no effect on the measurement.

Keratometry values are generated in 3 zones out of 18 spots in an area of about 3.2 mm for an 8 mm radius cornea. The system is designed to sample local irregularities in the central zone of the cornea into the final keratometry, which would not be possible with a ring measurement only. This 3-zone approach also allows for measurement of the central topography (see below). The keratometry measurement is repeated 15 times, with an algorithm detecting and erasing outliers and providing warnings to users in case of inconsistencies between single measurements or the different measurement rings. This telecen-

tric approach to keratometry has proven to be precise and repeatable in many studies. [4, 5, 9–17]

The **keratometric index** on the IOLMaster 700 can be chosen by the user to match individual requirements. The choice of keratometric index has no effect on IOL power calculation though, as for the internal calculation algorithms, only directly measured radii are used, which are unaffected by the keratometric index.

Additional Measurements

Angle Alpha- and Kappa-Chords

The ZEISS IOLMaster 700 measures the Subject Fixated—Coaxially Sighted Corneal Light Reflex (SF-CSCLR) as described by Chang and Waring [19], or corneal vertex, which gives an approximation of the position of the corneal intercept of the visual axis. It then displays the **chord of angle alpha** and the **chord of angle kappa**, as the angles (in degrees) cannot be measured directly. The chords are defined as the distance between the corneal vertex and the limbus center (alpha)/the pupil center (kappa). They are displayed either in cartesian (I_x/I_y and P_x, P_y , for alpha

and kappa, respectively) or polar coordinates (alpha (chord) and kappa (chord)/CW-Chord, respectively).

Corneal and Pupil Diameter

The horizontal corneal diameter and pupil diameter are measured from the image of the eye taken at 860–880 nm.

Total Keratometry: Replacing Assumptions with Measurements

Principle of Total Keratometry

A known limitation of classic keratometry is that the posterior surface of the cornea is not measured but considered via a keratometric index only. However, several studies have confirmed that posterior corneal astigmatism magnitude and axis orientation cannot be adequately predicted by measuring the anterior corneal curvature alone [20–22]. Therefore, nomograms and mathematical models have been created in order to predict the posterior surface astigmatism and optimize toric IOL power calculation [23–25]. Yet, these methods are based on theoretical assumptions of posterior corneal astigmatism and, therefore, generally cannot fully account for outliers and irregularities.

This led ZEISS to the development of technology able to measure, not estimate, the posterior curvature: **Total Keratometry (TK[®])** [22]. TK[®] considers measured corneal thickness and measured posterior corneal curvature in addition to the anterior corneal curvature measurements. It combines telecentric 3-Zone Keratometry of the ZEISS IOLMaster 700 with its SWEPT Source OCT cornea-to-retina scan [4, 11, 26].

TK[®] has been designed to match the Gullstrand ratio in normal eyes. However, it still can detect the impact of posterior astigmatism in individual eyes, such as eyes with post corneal laser vision correction. An additional significant advantage of this approach is that TK[®] can be directly incorporated in classic IOL power calculation

formulas, while using existing optimized IOL constants, such as ULIB and IOLCon [27, 28].

Precision of Total Keratometry Measurements

Goggin and LaHood first published data confirming that the ZEISS IOLMaster 700 is capable of measuring the posterior corneal surface [22]. Savini et al. [29] assessed the repeatability of TK[®] and standard keratometry measurements provided by ZEISS IOLMaster 700. They conclude that TK[®] measurements offer high repeatability in unoperated and post-excimer laser surgery eyes.

Clinical Results with Total Keratometry in Non-toric and Toric IOL Power Calculation

While TK[®] values are equivalent to K values in normal eyes, they will differ in eyes with an unusual ratio of anterior-to-posterior corneal curvature or in patients with an unusual posterior astigmatism. In these cases, the classic posterior corneal astigmatism nomograms cannot detect these outliers, while TK[®] can. Therefore, one can expect that TK[®] and K will overall perform relatively similar in terms of mean refractive outcomes after cataract surgery in normal eyes. However, TK[®] will be able to help surgeons avoid outliers or refractive surprises in the unusual cases mentioned above. Published studies by Fabian and Wehner or Srivannaboon and Chirapapaisan confirm this behavior with respect to spherical equivalent and cylinder prediction errors [27, 28].

Clinical Performance of Total Keratometry in Post-corneal Refractive Surgery Eyes

Eyes after refractive corneal laser surgery are the most prominent example of unusual anterior and posterior corneal curvature ratio, as the anterior surface has been altered. In these eyes,

TK[®] becomes very beneficial, as it does not rely on assumptions on the posterior surface but is a measurement of total corneal power taking actual posterior corneal curvatures into consideration.

Wang et al. have shown, for example, that TK[®] can be used in classic IOL power calculation formulas such as the Haigis formula, resulting in overall similar results like specifically designed post-LVC formulas as the Barrett True K without taking historical refraction data into account [30].

Lawless et al. have shown in their publication that when using the Barrett True K TK[®] formula,

which was specifically designed for TK[®], it outperformed any other non-history formula in post-myopic LASIK eyes evaluated in this study [31] (Fig. 17.3). They also confirm, that Haigis with TK provides similar results as Barrett True K with K and no history.

Yeo et al. analyzed in this open-access paper 64 eyes with previous myopic laser refractive surgery by comparing the prediction error on different formulas [32]. In their analysis, EVO with TK[®] followed by Barrett True-K TK[®] and Haigis with TK[®] achieved the highest percentages of patients with absolute prediction error within 0.50 and 1.00 D (Fig. 17.4).

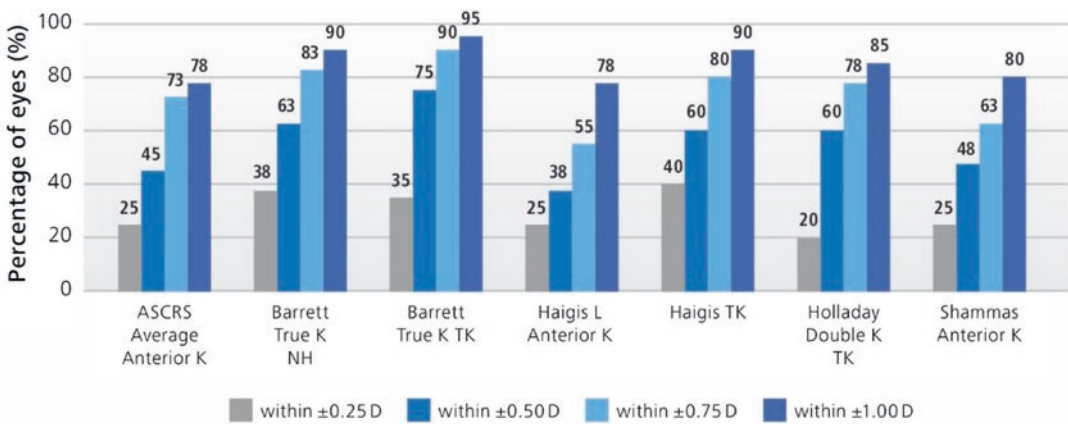


Fig. 17.3 Percentage of eyes within 0.25, 0.50, 0.75, and 1.00 D of absolute prediction error; no-history formulas followed by formulas using TK. (Taken from Lawless et al. 2020)

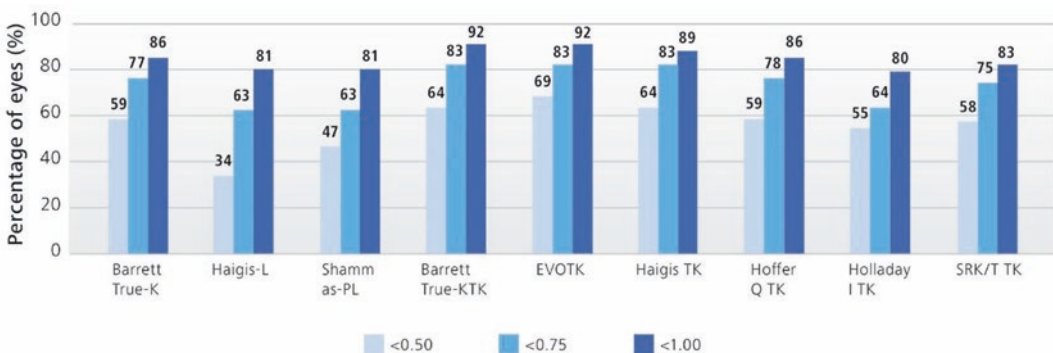


Fig. 17.4 Percentage of eyes within 0.50, 0.75, and 1.00 D of absolute prediction error. (Taken from Yeo et al. 2020)

Central Topography: Starting Your Workflow with More Insights

Central topography combines keratometry data from the 3-Zone Telecentric Keratometry with data of the corneal thickness measurement of the SWEPT Source OCT to create a **total axial power map** from the anterior and posterior corneal surface. This provides surgeons with more information on the central corneal shape right from the start without changing workflow or taking more time (Fig. 17.2).

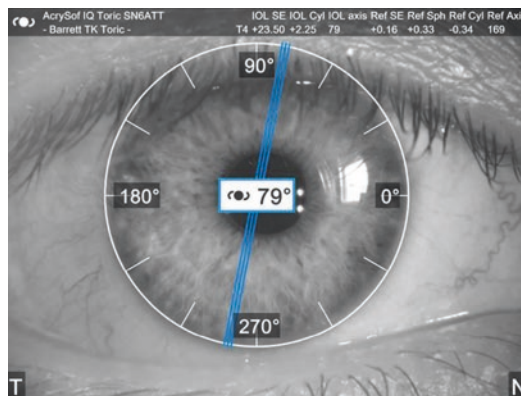
Wang et al. compared central topography maps to topographic maps from a Placido-dual-Scheimpflug Topographer. This study included 105 eyes with various corneal conditions such as regular/irregular corneas, previous corneal refractive surgery, and keratoconus or pellucid marginal degeneration. In 68.6–89.5%, similar overall shape was observed which leads to the same decision for premium IOL selection in 75.2–97.1% of cases [33].

Fig. 17.5 Example of IOLMaster 700 reference image with planned toric IOL, predicted refraction, formula information, and implantation axis information based on TK®

Markerless Toric IOL Alignment

The ZEISS IOLMaster 700 is able to acquire a red-free (520 nm) image of the limbal vessels and iris structures during the keratometry measurement.

Both reference image and keratometry data (Fig. 17.5) can be transferred to ZEISS CALLISTO® eye, e.g., together with your surgical planning from VERACITY® Surgical or EQ Workplace. During surgery, the image is then used for intraoperative matching with the live eye image. All data needed is displayed in the eyepiece or 3D screen of the surgical microscopes OPMI LUMERA® or ARTEVO® 800 from ZEISS. Preoperative corneal marking and additional measurements for Toric IOL alignment thus become obsolete. Solomon and Ladas conclude that within their study, the use of ZEISS CALLISTO® eye yields less remaining refractive cylinder than Toric IOL placement guided by intraoperative aberrometry [3].



IOL Power Calculation

The ZEISS IOLMaster 700 offers a broad range of formula to calculate IOLs for a wide range of eyes, from long to short eyes, including toric IOL power calculation (Fig. 17.6) and post-corneal refractive surgery IOL power calculation, including post-RK cases (Table 17.2).

The ZEISS IOLMaster 700 supports import of IOL power steps and ranges as well as constants from the IOLCon.org website. Download of IOL data directly from IOLCon.org is recommended to always have access to the latest and best optimized IOL data directly from the respective IOL manufacturer.

Fig. 17.6 ZEISS IOLMaster 700 toric IOL power calculation report

AcrySof SN6AT(2-9)

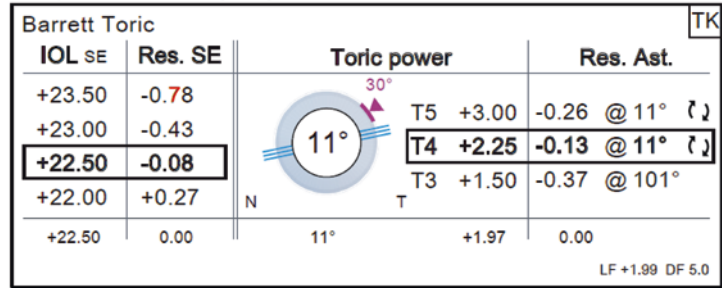


Table 17.2 IOL power calculation formulas available on ZEISS IOLMaster 700, ZEISS EQ Workplace, and ZEISS Veracity Surgical (June 2021)

Formula	K/TK	Non-toric	Toric	Post-refractive surgery	Post-refractive surgery toric	IOLMaster 700	EQ Workplace	Veracity Surgical Planner (US only)
Abulafia-Koch	K		•					•
SRK/T	K/TK®	•				•	•	•
Hoffer Q	K/TK®	•				•	•	•
Holladay	K/TK®	•				•	•	•
Holladay 1								
Holladay 2								
Haigis suite						•	•	
Haigis	K/TK®	•		• TK® only				
Haigis-T	K/TK®		•		• TK® only			
Haigis-L	K			•				
Haigis-L toric	K				•			
Barrett suite	K/TK®	•				•	•	•
Barrett universal II								
Barrett toric calculator			•					
Barrett true K				•				
Barrett true K toric					•			
Kane suite	K/TK®						• (2024)	•
Kane		•						
Kane toric			•					
Z CALC (ZEISS IOL only)	K/TK®	•	•	•	•		•	

ZEISS Cataract Workflow

ZEISS offers a selection of software solutions to complement the ZEISS IOLMaster 700 and help cataract surgeons to streamline their cataract workflow. From a wider selection of formulas, remote IOL power calculation, remote surgery planning, constant optimization, IOL ordering to postop quality assessment. Those will be addressed in the following chapter: ZEISS Cataract Workflow.

References

1. Montés-Micó R, Pastor-Pascual F, Ruiz-Mesa R, Tañá-Rivero P. Ocular biometry with swept-source optical coherence tomography. *J Cataract Refract Surg.* 2021;47:802–14.
2. Mayer WJ, Kreutzer T, Dirisamer M, Kern C, Kortuem K, Vounotrypidis E, Priglinger S, Kook D. Comparison of visual outcomes, alignment accuracy, and surgical time between 2 methods of corneal marking for toric intraocular lens implantation. *J Cataract Refract Surg.* 2017;43:1281.
3. Solomon JD, Ladas J. Toric outcomes: computer-assisted registration versus intraoperative aberrometry. *J Cataract Refract Surg.* 2017;43:498.
4. Srivannaboon S, Chirapapaisan C, Chonpimai P, Loket S. Clinical comparison of a new swept-source optical coherence tomography-based optical biometer and a time-domain optical coherence tomography-based optical biometer. *J Cataract Refract Surg.* 2015;41:2224–32.
5. Sel S, Stange J, Kaiser D, Kiraly L. Repeatability and agreement of Scheimpflug-based and swept-source optical biometry measurements. *Contact Lens Anterior Eye.* 2017;40:318.
6. Yang JY, Kim HK, Kim SS. Axial length measurements: comparison of a new swept-source optical coherence tomography-based biometer and partial coherence interferometry in myopia. *J Cataract Refract Surg.* 2017;43:328.
7. Passi SF, Thompson AC, Gupta PK. Comparison of agreement and efficiency of a swept source-optical coherence tomography device and an optical low-coherence reflectometry device for biometry measurements during cataract evaluation. *Clin Ophthalmol.* 2018;12:2245.
8. Carl Zeiss Meditec, Clinical Trial, IOLMaster 700-2015-1.
9. Shetty N, Kaweri L, Koshy A, Shetty R, Nuijts RMMA, Sinha Roy A. Repeatability of biometry measured by three devices and its impact on predicted intraocular lens power. *J Cataract Refract Surg.* 2021;47:585–92.
10. Kurian M, Negalur N, Das S, Puttaiah NK, Haria D, Tejal SJ, Thakkar MM. Biometry with a new swept-source optical coherence tomography biometer: repeatability and agreement with an optical low-coherence reflectometry device. *J Cataract Refract Surg.* 2016;42:577–81.
11. Kunert KS, Peter M, Blum M, Haigis W, Sekundo W, Schütze J, Bühren T. Repeatability and agreement in optical biometry of a new swept-source optical coherence tomography-based biometer versus partial coherence interferometry and optical low-coherence reflectometry. *J Cataract Refract Surg.* 2016;42:76–83.
12. Martínez-Albert N, Esteve-Taboada JJ, Montés-Micó R, Fernández-Vega-Cueto L, Ferrer-Blasco T. Repeatability assessment of biometric measurements with different refractive states and age using a swept-source biometer. *Expert Rev Med Devices.* 2019;16:63–9.
13. Jung S, Chin HS, Kim NR, Lee KW, Jung JW. Comparison of repeatability and agreement between swept-source optical biometry and dual-Scheimpflug topography. *J Ophthalmol.* 2017;2017:1516395.
14. Garza-Leon M, La Fuentes-de Fuente HA, García-Treviño AV. Repeatability of ocular biometry with IOLMaster 700 in subjects with clear lens. *Int Ophthalmol.* 2017;37:1133–8.
15. Bullimore MA, Slade S, Yoo P, Otani T. An evaluation of the IOLMaster 700. *Eye Contact Lens.* 2019;45:117.
16. Huang J, Zhao Y, Savini G, Yu G, Yu J, Chen Z, Tu R, Zhao Y. Reliability of a new swept-source optical coherence tomography biometer in healthy children, adults, and cataract patients. *J Ophthalmol.* 2020;2020:8946364.
17. Chan TCY, Wan KH, Tang FY, Wang YM, Yu M, Cheung C. Repeatability and agreement of a swept-source optical coherence tomography-based biometer IOLMaster 700 versus a Scheimpflug imaging-based biometer AL-scan in cataract patients. *Eye Contact Lens.* 2020;46:35–45.
18. Hirschall N, Varsits R, Doeller B, Findl O. Enhanced penetration for axial length measurement of eyes with dense cataracts using swept source optical coherence tomography: a consecutive observational study. *Ophthalmol Therapy.* 2018;7:119.
19. Chang DH, Waring GO. The subject-fixated coaxially sighted corneal light reflex: a clinical marker for centration of refractive treatments and devices. *Am J Ophthalmol.* 2014;158:863–874.e2.
20. Tonn B, Klaproth OK, Kohnen T. Anterior surface-based keratometry compared with scheimpflug tomography-based total corneal astigmatism. *Investig Ophthalmol Vis Sci.* 2014;56:291.
21. Koch DD, Ali SF, Weikert MP, Shirayama M, Jenkins R, Wang L. Contribution of posterior corneal astigmatism to total corneal astigmatism. *J Cataract Refract Surg.* 2012;38:2080.

22. LaHood BR, Goggin M. Measurement of posterior corneal astigmatism by the IOLmaster 700. *J Refract Surg.* 2018;34:331.
23. Koch DD, Jenkins RB, Weikert MP, Yeu E, Wang L. Correcting astigmatism with toric intraocular lenses: effect of posterior corneal astigmatism. *J Cataract Refract Surg.* 2013;39:1803–9.
24. Abulafia A, Koch DD, Wang L, Hill WE, Assia EI, Franchina M, Barrett GD. New regression formula for toric intraocular lens calculations. *J Cataract Refract Surg.* 2016;42:663–71.
25. Canovas C, Alarcon A, Rosén R, Kasthurirangan S, Ma JJK, Koch DD, Piers P. New algorithm for toric intraocular lens power calculation considering the posterior corneal astigmatism. *J Cataract Refract Surg.* 2018;44:168–74.
26. Akman A, Asena L, Güngör SG. Evaluation and comparison of the new swept source OCT-based IOLMaster 700 with the IOLMaster 500. *Br J Ophthalmol.* 2016;100:1201–5.
27. Fabian E, Wehner W. Prediction accuracy of total keratometry compared to standard keratometry using different intraocular lens power formulas. *J Refract Surg.* 2019;35:362.
28. Srivannaboon S, Chirapapaisan C. Comparison of refractive outcomes using conventional keratometry or total keratometry for IOL power calculation in cataract surgery. *Graefe's archive for clinical and experimental ophthalmology. Albrecht Von Graefes Arch Klin Exp Ophthalmol.* 2019;257:2677–82.
29. Savini G, Taroni L, Schiano-Lomoriello D, Hoffer KJ. Repeatability of total Keratometry and standard Keratometry by the IOLMaster 700 and comparison to total corneal astigmatism by Scheimpflug imaging. *Eye (London, England).* 2020;35:307.
30. Wang L, Spektor T, de Souza RG, Koch DD. Evaluation of total keratometry and its accuracy for intraocular lens power calculation in eyes after corneal refractive surgery. *J Cataract Refract Surg.* 2019;45:1416–21.
31. Lawless M, Jiang JY, Hodge C, Sutton G, Roberts TV, Barrett G. Total keratometry in intraocular lens power calculations in eyes with previous laser refractive surgery. *Clin Exp Ophthalmol.* 2020;48:749–56.
32. Yeo TK, Heng WJ, Pek D, Wong J, Fam HB. Accuracy of intraocular lens formulas using total keratometry in eyes with previous myopic laser refractive surgery. *Eye.* 2020;35:1705.
33. Wang L, Canedo ALC, Wang Y, Xie KC, Koch DD. Comparison of central topographic maps from a swept-source OCT biometer and a Placido disk-dual Scheimpflug tomographer. *J Cataract Refract Surg.* 2021;47:482–7.

Open Access This chapter is licensed under the terms of the Creative Commons Attribution 4.0 International License (<http://creativecommons.org/licenses/by/4.0/>), which permits use, sharing, adaptation, distribution and reproduction in any medium or format, as long as you give appropriate credit to the original author(s) and the source, provide a link to the Creative Commons license and indicate if changes were made.

The images or other third party material in this chapter are included in the chapter's Creative Commons license, unless indicated otherwise in a credit line to the material. If material is not included in the chapter's Creative Commons license and your intended use is not permitted by statutory regulation or exceeds the permitted use, you will need to obtain permission directly from the copyright holder.

